



AFRL-RY-HS-TR-2010-0036

---

A Realistic Theoretical Model for Laminar Flow over a Flat Plate

David W. Weyburne

AFRL/RYHC  
80 Scott Drive  
Hanscom AFB, MA 01731-2909

14 September 2010

Technical Report

APPROVED FOR PUBLIC RELEASE; DISTRIBUTION UNLIMITED

AIR FORCE RESEARCH LABORATORY  
Sensors Directorate  
Electromagnetics Technology Division  
Hanscom AFB MA 01731-2909

## NOTICE AND SIGNATURE PAGE


Using Government drawings, specifications, or other data included in this document for any purpose other than Government procurement does not in any way obligate the U.S. Government. The fact that the Government formulated or supplied the drawings, specifications, or other data does not license the holder or any other person or corporation; or convey any rights or permission to manufacture, use, or sell any patented invention that may relate to them.

This report was cleared for public release by the Electronic Systems Center Public Affairs Office for the Air Force Research Laboratory Electromagnetic Technology Division and is available to the general public, including foreign nationals. Copies may be obtained from the Defense Technical Information Center (DTIC) (<http://www.dtic.mil>).

AFRL-RY-HS-TR-2010- 0036 HAS BEEN REVIEWED AND IS APPROVED FOR PUBLICATION IN ACCORDANCE WITH ASSIGNED DISTRIBUTION STATEMENT.



DAVID WEYBURNE  
Contract Monitor



DAVID F. BLISS, Acting Chief  
Optoelectronic Technology Branch



ROBERT V. McGAHAN  
Technical Communications Advisor  
Electromagnetics Technology Division

This report is published in the interest of scientific and technical information exchange, and its publication does not constitute the Government's approval or disapproval of its ideas or findings.

REPORT DOCUMENTATION PAGE				Form Approved OMB No. 0704-0188	
Public reporting burden for this collection of information is estimated to average 1 hour per response, including the time for reviewing instructions, searching existing data sources, gathering and maintaining the data needed, and completing and reviewing this collection of information. Send comments regarding this burden estimate or any other aspect of this collection of information, including suggestions for reducing this burden to Department of Defense, Washington Headquarters Services, Directorate for Information Operations and Reports (0704-0188), 1215 Jefferson Davis Highway, Suite 1204, Arlington, VA 22202-4302. Respondents should be aware that notwithstanding any other provision of law, no person shall be subject to any penalty for failing to comply with a collection of information if it does not display a currently valid OMB control number. <b>PLEASE DO NOT RETURN YOUR FORM TO THE ABOVE ADDRESS.</b>					
1. REPORT DATE (DD-MM-YYYY) 14-09-2010		2. REPORT TYPE TECHNICAL REPORT		3. DATES COVERED (From - To) 1 JAN 2010 – 1 SEPT 2010	
4. TITLE AND SUBTITLE  A Realistic Theoretical Model for Laminar Flow over a Flat Plate				5a. CONTRACT NUMBER IN-HOUSE	
				5b. GRANT NUMBER	
				5c. PROGRAM ELEMENT NUMBER 62204F	
6. AUTHOR(S)  David W. Weyburne				5d. PROJECT NUMBER 4916	
				5e. TASK NUMBER HC	
				5f. WORK UNIT NUMBER 10	
7. PERFORMING ORGANIZATION NAME(S) AND ADDRESS(ES)  AFRL/RYHC 80 Scott Drive Hanscom AFB, MA 01731-2909				8. PERFORMING ORGANIZATION REPORT NUMBER	
9. SPONSORING / MONITORING AGENCY NAME(S) AND ADDRESS(ES) Electromagnetics Technology Division Sensors Directorate Air Force Research Laboratory 80 Scott Drive Hanscom AFB, MA 01731-2909				10. SPONSOR/MONITOR'S ACRONYM(S) AFRL/RYHC	
				11. SPONSOR/MONITOR'S REPORT NUMBER(S) AFRL-RY-HS-TR-2010-0036	
12. DISTRIBUTION / AVAILABILITY STATEMENT  DISTRIBUTION A: APPROVED FOR PUBLIC RELEASE: DISTRIBUTION UNLIMITED					
13. SUPPLEMENTARY NOTES The U.S. Government is joint author of this work and has the right to use, modify, reproduce, release, perform, display, or disclose the work.					
14. ABSTRACT The problem of theoretically describing forced laminar flow over a flat plate is revisited. For the last hundred years it has been assumed that the Blasius solution model applies to this case. However, upon close review it is found that the Blasius model has a serious problem in that the Blasius model assumes that the pressure gradient on the plate in the flow direction is zero. In fact what one expects is that a pressure gradient develops as fluid is displaced from the plate due to the developing boundary layer. Therefore, the Blasius model is not a valid physical model of the flow over a flat plate as depicted in most textbooks. In this report, we develop a more realistic Falkner-Skan type similar solution that closely matches the flow one would expect for flow over a flat plate. We replace the usual zero pressure gradient assumption with a nonzero pressure gradient assumption. The resulting solution for the velocity profile parallel to the plate results in a velocity profile that is very similar to the Blasius solution velocity profile. The big difference in the two models is in the velocity perpendicular to the plate. For the Blasius solution, this velocity results in a net outflow whereas the new model's velocity results in a net inflow. This net inflow is critical in that it allows one to use the flat plate as a model for a wing with aerodynamic lift.					
15. SUBJECT TERMS Fluid Boundary Layer, Blasius Model, Laminar Flow, Aerodynamic Lift, Flat Plate					
16. SECURITY CLASSIFICATION OF:			17. LIMITATION OF ABSTRACT  SAR	18. NUMBER OF PAGES  23	19a. NAME OF RESPONSIBLE PERSON David W. Weyburne
a. REPORT Unclassified	b. ABSTRACT Unclassified	c. THIS PAGE Unclassified			19b. TELEPHONE NUMBER N/A





## Contents

List of Figures .....	iv
Acknowledgments .....	v
Summary .....	1
1. Introduction .....	2
2. $x$ -momentum Balance Equation .....	3
3. Variable Transform .....	4
4. Dimensionless Momentum Equation .....	4
5. Laminar Flow Similarity Equation .....	5
6. Boundary Conditions .....	6
7. A Realistic Similarity Solution for a Flat Plate .....	7
7.1 Scenario 1 .....	8
7.2 Scenario 2 .....	10
7.2 Scenario 3 .....	10
8. Discussion .....	11
9. Conclusion .....	13
References .....	13

## List of Figures

- Figure 1. The crosses are the calculated results from Eq. 17 for  $m$  versus  $\eta_{v0}$ . The blue line is added as a guide to the eye. .... 7
- Figure 2. The calculated results from Eq. 17 for  $f$ ,  $f'$ , and  $f''$  with  $m=0$  and  $m=0.1356$ . The  $x$ -axis values for the  $m=0.1356$  case are multiplied by 1.31 to properly compare the two solutions. .... 8
- Figure 3. The calculated results from Eq. 17 for  $u/u_e$  with  $m=0$  and  $m=0.1356$ . The  $x$ -axis values for the  $m=0.1356$  case are multiplied by 1.31 to properly compare the two solutions. .... 9
- Figure 4. The calculated results from Eq. 17 for the scaled  $v(x,y)$  with  $m=0$  and  $m=0.1356$ . The  $x$ -axis values for the  $m=0.1356$  case are multiplied by 1.31 to properly compare the two solutions. .... 9
- Figure 5. The calculated results from Eq. 17 for  $f$ ,  $f'$ , and  $f''$  with  $m=0$  and  $m=0.05226$ . The  $x$ -axis values for the  $m=0.05226$  case are multiplied by 1.31 to properly compare the two solutions. .... 8
- Figure 6. The calculated results from Eq. 17 for  $u/u_e$  with  $m=0$  and  $m=0.05226$ . The  $x$ -axis values for the  $m=0.05226$  case are multiplied by 1.31 to properly compare the two solutions. .... 9
- Figure 7. The calculated results from Eq. 17 for the scaled  $v(x,y)$  with  $m=0$  and  $m=0.05226$ . The  $x$ -axis values for the  $m=0.05226$  case are multiplied by 1.31 to properly compare the two solutions. .... 9
- Figure 8. The calculated results from Eq. 17 for  $f$ ,  $f'$ , and  $f''$  with  $m=0$  and  $m=0.008448$ . The  $x$ -axis values for the  $m=0.008448$  case are multiplied by 1.039 to properly compare the two solutions. .... 10
- Figure 9. The calculated results from Eq. 17 for the scaled  $v(x,y)$  with  $m=0$  and  $m=0.008448$ . The  $x$ -axis values for the  $m=0.008448$  case are multiplied by 1.039 to properly compare the two solutions. .... 10

### **Acknowledgement**

The author would like to acknowledge the support of the Electromagnetics Technology Division of the Sensors Directorate of the Air Force Research Laboratory.



## 1. Introduction

The Blasius [1] model for laminar flow over a flat plate has been a cornerstone of fluid flow theory for more than a hundred years. Wind tunnel results have consistently shown very good correspondence between the Blasius solution and experimental findings (see for example [2,3]). Although the Blasius solution is numerical in nature (as opposed to an analytical solution), the simplicity of the Blasius differential equation and its numerical solution are such that the result is universally considered an exact result of the flow-governing equations. However, a close look at the Blasius model reveals a disturbing discrepancy from what one would expect for flow over a flat plate. The problem with the Blasius model has to do with the pressure gradient assumed for this flow situation. The Blasius model assumes a zero pressure gradient in the flow direction along the plate. In fact, what one would expect for flow over a flat plate is that a pressure gradient would develop along the plate as fluid is displaced from the plate surface due to the boundary layer. This pressure gradient would increase as one travels down the plate due simply to the fact that the boundary layer thickness, and hence the displaced fluid, increases as one moves along the plate. It is apparent, therefore, that the Blasius model does not match up with our expectation for flow over a flat plate. Therefore, while the Blasius "solution" is a valid mathematical solution to a certain flow situation, it is not a valid solution to the flow governing equations for flow over a flat plate as depicted in most textbooks.

Clearly the Blasius model has a problem, but in the past this problem has been dismissed as a small anomaly that occurs when one tries to apply a very simple theoretical model to a real fluid. In support of the Blasius model, one can always point to the numerous wind tunnel-based experimental papers in which the measurement of the Blasius velocity profile is now used to verify that the wind tunnel is configured properly for laminar flow (see for example [2,3]). It turns out that is relatively easy to set up a wind tunnel to achieve a zero pressure gradient along the plate. However, it is very instructive to see how the zero pressure gradient is established. Consider the paper by Jovanović, *et. al.* [2] for example. In order to obtain a zero pressure gradient at the LSTM wind tunnel in Erlangen, the flat plate is mounted on a turntable which is located in the floor of the measuring section. The angle of attack of the plate is adjusted until the largest possible constant pressure area in the flow direction is obtained. Note that by adjusting the angle of attack away from zero degrees, one is imposing a pressure gradient on the flow which is used to counter act the built-in pressure gradient that develops due to fluid displacement in the boundary layer. This results in a nearly zero pressure gradient. The paper by Patten, Young, and Griffin [3] is another example where wind tunnel qualification is done by measuring Blasius velocity profiles. In this case, the pressure gradient along the plate in the University of Limerick's wind tunnel was adjusted by a trailing edge flap. The flap was manipulated until the largest possible constant pressure area in the flow direction was obtained, which occurred for a flap setting of 40°. Here again, an external pressure gradient, this time created by the trailing edge flap, is used to counter act the built-in pressure gradient due to the boundary layer. These two examples illustrate that it is possible to experimentally generate flows which match the Blasius model. However, it is also clear from these manipulations necessary to produce Blasius flows that the Blasius model does not represent the flow depicted in most textbooks for flow over a flat plate.

The intent of this paper is to develop a theoretical model that more closely matches what is expected for flow over a flat plate. In order to develop this model it is important to review what one would expect for flow over a flat plate. As already discussed above, what we would expect for flow along the plate is that a pressure gradient would develop and increase along the



plate as more and more fluid is displaced from the plate surface due to the increasing thickness of the boundary layer along the plate. This pressure gradient extends well beyond the boundary layer into the inviscid region above the plate surface. The pressure gradient along the plate will induce a higher boundary layer edge velocity which in turn will induce a net inward velocity (toward the plate) at some point in the free stream above the plate due to conservation of mass. Therefore, a more realistic model for flow over a flat plate is to assume 1) a small nonzero pressure gradient develops along the flow direction and that 2) the velocity perpendicular to the plate starts out as an outflow and then becomes an inflow at some point above the plate. From an aerodynamic stand point, this net inflow allows one to begin to explain the origin of lift using a flat plate as a model for a wing.

In what follows we show that it is possible to develop a more realistic theoretical model for flow over a flat plate that still retains the simplicity of the Blasius model. In particular, in the model proposed below the usual zero pressure gradient assumption is removed and replaced with a nonzero pressure gradient assumption. This allows one to obtain a Falkner-Skan-type [4] similarity solution to the momentum equation. The Falkner-Skan similarity solution is usually associated with flow around a wedge but it is equally correct to interpret the equations in terms of flow on a flat plate with a pressure gradient. The resulting differential equation is similar to the Blasius equation and is easily solved with a shooting-Runge-Kutta method. By adjusting the strength of the pressure gradient, the velocity perpendicular to the plate can be made to go from positive to negative at a point above the plate. The resulting solution for the velocity profile parallel to the plate results in a solution that is almost indistinguishable from the Blasius solution for the scaled velocity profile  $u(x, y)$  where  $u(x, y)$  is the velocity parallel to the plate.

## 2. $x$ -momentum Balance Equation

To begin our development, we first establish the relevant flow governing equations for 2-D laminar flow over a flat plate. Laminar flow past a flat plate can be modeled theoretically by a combination of the Navier-Stokes equation and the continuity equation. Assume that the  $x$ -axis is placed in the plane of the flat plate, that the  $y$ -axis is at right angles to the flat plate's top surface, and the  $z$ -axis is along the leading edge of the plate. The velocity  $u$  is the velocity parallel to the plate ( $x$ -direction) and the velocity  $v$  is the velocity perpendicular to the plate ( $y$ -direction). Both are in general a function of  $x$  and  $y$ . A steady flow parallel to the  $x$ -axis impinges the flat plate with a velocity  $u_\infty$  that is constant. We follow tradition and make the usual boundary layer approximations (see for example, Schlichting [5]). Furthermore, only steady state solutions are considered. For a 2-D, incompressible, constant property, laminar boundary layer on a flat plate, the  $x$ -component of the momentum balance is given approximately by

$$u \frac{\partial u}{\partial x} + v \frac{\partial u}{\partial y} \cong -\frac{1}{\rho} \frac{\partial p}{\partial x} + \nu \frac{\partial^2 u}{\partial y^2} \quad , \quad (1)$$

where  $\rho$  is the density,  $\nu$  is the kinematic viscosity, and  $p$  is the pressure. The equation for the mass conservation requires

$$\frac{\partial u}{\partial x} + \frac{\partial v}{\partial y} = 0 \quad . \quad (2)$$

These equations are considered exact within the normal boundary layer considerations.

### 3. Variable Transform

The solution to Eqs. 1 and 2 begins with a variable transformation to nondimensionalize the equations. In order to reduce the equations to dimensionless equations we start by introducing the independent variables  $\xi$  and  $\eta$  given by

$$\xi = x, \quad \eta = \frac{y}{\delta(x)}, \quad (3)$$

where the function  $\delta(x)$  is the as yet unspecified boundary layer thickness which is a function of  $x$ . Furthermore, we define a stream function  $\psi(x, y)$  in terms of a dimensionless function  $f(\xi, \eta)$  as

$$\frac{\psi(x, y)}{\delta(x)u_s(x)} = f(\xi, \eta), \quad (4)$$

where  $u_s(x)$  is the as yet unspecified scaling velocity. The stream function satisfies the conditions

$$u = \frac{\partial \psi(x, y)}{\partial y}, \quad v = -\frac{\partial \psi(x, y)}{\partial x}. \quad (5)$$

This means that

$$v = -\frac{d\{\delta u_s\}}{dx}f + u_s \frac{\partial \delta}{\partial x} \eta f' - \delta u_s \frac{\partial f}{\partial \xi}, \quad (6)$$

where the prime indicates differentiation with respect to  $\eta$ , and where we have used the fact that

$$\frac{\partial \eta}{\partial x} = \frac{\partial}{\partial x} \left\{ \frac{y}{\delta(x)} \right\} = -\frac{\eta}{\delta} \frac{d\delta}{dx} \quad (7)$$

and that

$$\frac{\partial \eta}{\partial y} = \frac{\partial}{\partial y} \left\{ \frac{y}{\delta(x)} \right\} = \frac{1}{\delta}. \quad (8)$$

The velocity in the  $x$ -direction is given by

$$u = u_s f', \quad (9)$$

where we have used the fact that  $\frac{\partial \xi}{\partial y} = 0$ . It is easily verified that these velocity definitions, Eqs. 6 and 9, satisfy the continuity equation (Eq. 2).

### 4. Dimensionless Momentum Equation

Substituting the above dimensionless variables into the  $x$ -component of the momentum equation (Eq. 1), starting on the left-hand side of the equation, we have

$$u \frac{\partial u}{\partial x} = u_s \frac{du_s}{dx} f'^2 - \frac{u_s^2}{\delta} \frac{d\delta}{dx} \eta f' f'' + u_s^2 f' \frac{\partial f'}{\partial \xi}. \quad (10)$$

The next term becomes



$$v \frac{\partial u}{\partial y} = -\frac{u_s}{\delta} \frac{d\{\delta u_s\}}{dx} ff'' + \frac{u_s^2}{\delta} \frac{\partial \delta}{\partial x} \eta f' f'' - u_s^2 f'' \frac{\partial f}{\partial \xi} \quad (11)$$

Combining these terms we have

$$\left\{ u \frac{\partial u}{\partial x} + v \frac{\partial u}{\partial y} \right\} = u_s \frac{du_s}{dx} f'^2 - \frac{u_s}{\delta} \frac{d\{\delta u_s\}}{dx} ff'' + u_s^2 f' \frac{\partial f'}{\partial \xi} - u_s^2 f'' \frac{\partial f}{\partial \xi} \quad (12)$$

The next step is to transform the viscous component in Eq. 1 given by

$$v \frac{\partial^2 u}{\partial y^2} = v \frac{u_s}{\delta^2} f''' \quad (13)$$

The transformed momentum equation (Eq. 1) therefore reduces to

$$u_s \frac{du_s}{dx} f'^2 - \frac{u_s}{\delta} \frac{d\{\delta u_s\}}{dx} ff'' + u_s^2 f' \frac{\partial f'}{\partial \xi} - u_s^2 f'' \frac{\partial f}{\partial \xi} \cong -\frac{1}{\rho} \frac{\partial p}{\partial x} + v \frac{u_s}{\delta^2} f''' \quad (14)$$

This equation is considered exact within the normal boundary layer considerations as discussed above.

### 5. Laminar Flow Similarity Equation

In order to solve Eq. 14, we make the assumption that the terms involving differentiation with respect to  $\xi$  are negligible. To find similar solutions, we need functional forms for  $u_s$  and  $\delta$ . The velocity  $u_s$  is taken to be the velocity at the boundary layer edge  $u_e$  which is not in general the inlet velocity  $u_\infty$ . For the boundary layer thickness we assume a Blasius-like value given by

$$\delta(x) = a \sqrt{v(x-x_0)/u_e} \quad (15)$$

where  $a$  and  $x_0$  are constants but with the caveat that  $u_e$  is allowed to be a function of  $x$ . For the pressure gradient we use the Bernoulli's equation,

$$-\frac{1}{\rho} \frac{\partial p}{\partial x} = u_e \frac{du_e}{dx} \quad (16)$$

Under these conditions, the  $x$ -momentum equation (Eq. 14) reduces to

$$\frac{f'''}{a^2} + \frac{ff''}{2} + m \left( 1 - f'^2 + \frac{ff''}{2} \right) = 0 \quad (17)$$

where

$$m = \frac{x-x_0}{u_e} \frac{du_e}{dx} = -\frac{x-x_0}{\rho u_e^2} \frac{dp}{dx} \quad (18)$$

This dimensionless  $x$ -component momentum equation (Eq. 17) is, of course, essentially identical to the equation first developed by Falkner-Skan [4] for laminar flow over a wedge. It is apparent that the only way for this to lead to an equation that is free of any  $x$ -dependency, we must have  $m$  be a constant. In this case, Eq. 18 has a solution given by

$$u_e = b(x-x_0)^m \quad (19)$$



where  $b$  is a constant. For  $m=0$  and  $a=1$ , Eq. 17 reduces to the Blasius [1] equation for laminar flow over a flat plate. For  $m=1$  and  $a=1$ , this equation reduces to the Hiemenz [6] equation for laminar 2-D stagnation point flow.

## 6. Boundary Conditions

To solve Eq. 17, we need to consider the boundary conditions for this flow situation. For flow over a flat plate, the upper boundary layer condition on  $u$  requires that as  $y \rightarrow \infty$ :  $u \rightarrow u_e$ . This condition implies

$$u(x, y \rightarrow \infty) = u_e \Rightarrow f'(\xi, \eta \rightarrow \infty) = 1 \quad (20)$$

The no-slip wall boundary conditions on  $u$  and  $v$  require that as  $y \rightarrow 0$ :  $u \rightarrow 0, v \rightarrow 0$ . Since we are assuming the terms involving differentiation with respect to  $\xi$  are negligible, these conditions imply

$$u(x, y \rightarrow 0) = 0 \Rightarrow f'(\xi, \eta \rightarrow 0) = 0 \quad (21)$$

$$v(x, y \rightarrow 0) = -\frac{d\{\delta u_s\}}{dx} f + u_s \frac{\partial \delta}{\partial x} \eta f' = 0$$

$\Downarrow$

$$f(\xi, \eta \rightarrow 0) = 0$$

Using the three boundary conditions given by Eqs. 20 and 21, Eq. 17 is easily solved using a shooting-Runge-Kutta method.

The dimensionless velocity  $v(x, y)$  for laminar flow (Eq. 6) becomes

$$\frac{v(x, y)}{u_e \frac{\partial \delta}{\partial x}} \cong -\frac{1+m}{1-m} f + \eta f' \quad (22)$$

From the numerical solution of the Blasius model, this velocity component in the free stream asymptotes to a nonzero value given by

$$v(x, y)|_{y \rightarrow \infty} = 0.86039 u_\infty \sqrt{\frac{v}{x u_\infty}} \quad (23)$$

This means that for the Blasius model, there is a net outflow from the plate surface. On the other hand, for laminar flow over a flat plate, we would expect that the displacement of the fluid to result in the development of a pressure gradient which in turn results in a net inflow toward the plate surface for positive  $m$  values. Therefore, Eq. 22 must become zero and then negative at some point above the plate. Assuming this occurs in the inviscid region above the plate, then the  $v(x, y)$  becomes zero when

$$f(\xi, \eta)|_{v=0} = \frac{1-m}{1+m} \eta \quad (24)$$

From Eqs. 22 and 24, it is apparent that in the inviscid region above the plate,  $v(x, y)$  behaves linearly with  $\eta$  (or  $y$ ) and must have a negative slope since  $v(x, y)$  starts out positive for  $\eta$  small. This means that for  $m \neq 0$  and  $y \rightarrow \infty$ , then  $v(x, y) \rightarrow -\infty$ .

## 7. A Realistic Similarity Solution for a Flat Plate

The intent in this section is to find numerical similar solutions to the flow governing equations that more closely matches the expected flow behavior for laminar flow over a flat plate. For laminar flow on a flat plate case, the free stream velocity at the boundary edge is usually assumed to be constant and the pressure gradient is assumed to be zero. However, under these conditions, it is apparent that there is an outflow perpendicular to the plate that extends to infinity. One way to counter this outflow is to relax the conditions on the free stream velocity at the boundary edge and the pressure gradient along the plate. In particular, we will assume that the pressure gradient is nonzero and that the free stream velocity at the boundary edge changes

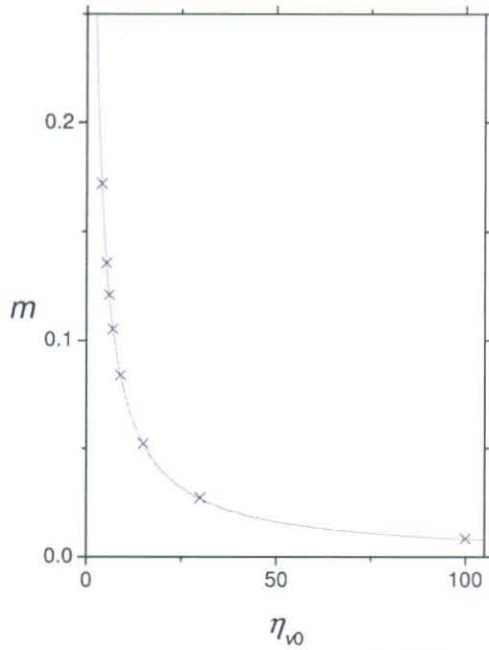


Fig. 1: The calculated  $m$  (Eq. 17) versus  $\eta_{v0}$ .

along the flow direction on the plate. This is equivalent to allowing the value of  $m$  in Eq. 17 to be nonzero. By allowing a pressure gradient to develop along the plate, it will be possible to insure that the velocity  $v(x, y)$  goes to zero at some finite location above the plate.

The solution strategy is to solve Eq. 17 for a specific  $m$  value and then calculate the scaled  $v(x, y)$  velocity using Eq. 22. By modifying a shooting-Runge-Kutta program that was used to solve the  $m=0$ ,  $a=1$  case, it is very straightforward to solve Eq. 17 for a specific nonzero  $m$  value. To keep the solution consistent with all the other reported Blasius solutions, we used  $a=1$  in all the calculations discussed herein. In solving Eq. 17, one finds that for a given value of  $m$ , the velocity given by Eq. 22 becomes zero at some finite  $\eta$  value which we will denote as  $\eta_{v0}$ . In Fig. 1, we show the plot of  $m$  versus  $\eta_{v0}$ . The calculated values are denoted by  $x$  and the fitted blue line, given by  $m = 1/(0.9418 + 1.2177\eta_{v0})$ , is added as a guide

to the eyes.

If the numerical solution procedure is used to solve Eq. 17 for a value of  $\eta$  that exceeds this  $\eta_{v0}$  value, then one finds that the velocity calculated by Eq. 22 becomes negative as discussed in Section 6 above. In the work reported herein, we arbitrarily choose to only calculate  $v(x, y)$  such that the maximum  $\eta$  value used in our numerical solution is given by  $\eta_{\max} = \eta_{v0} + 2$ . The point here is to emphasize the negative values but also make it clear that choosing this value for  $\eta_{\max}$  is arbitrary and that, in fact, for  $m \neq 0$  and  $\eta_{\max} \rightarrow \infty$ , then  $v(x, y) \rightarrow -\infty$ .

For real fluids, it is not clear where  $v(x, y)$  becomes zero since there is no experimental data available. We therefore picked three possible scenarios. The first corresponds to the case where  $v(x, y)$  becomes zero just above the top of the  $u(x, y)$  boundary layer. The second and



third cases correspond to more likely scenarios in which  $v(x, y)$  becomes zero many boundary layer thicknesses into the free stream above the plate.

### 7.1 Scenario 1

In the first scenario we assumed that  $v(x, y)$  becomes zero at  $\eta_{v0} \cong 5.29$  (which corresponds to the Blasius boundary layer thickness). Eq. 17 was then solved by hand iterating the  $m$  value until the scaled  $v(x, y)$  velocity given in Eq. 22 is zero at  $\eta_{v0}$ . It was found that this occurred at  $m=0.1356$ . The results are shown in Figs. 2-4. For comparison, the Blasius solution is also shown. In making the comparison, it is necessary to scale one or the other solution so that they have the same boundary layer thickness. In Figs. 2-4, the  $m=0.1356$  solution  $\eta$  values are scaled such that the scaled boundary thickness value, given by  $a$  in Eq. 15, is the same as the boundary thickness of the Blasius solution (the scaled boundary layer thickness was calculated according to Weyburne [7]). The scaled boundary layer thickness ratio was found to be 1.31. In Figs. 2-4, the  $m=0.1356$  solutions  $\eta$  values were multiplied by this 1.31 value. (Note that Figs. 2-4 alternate with Scenario 2's Figs. 5-7 so a side-by-side comparison is possible).

The velocity profile  $u/u_e$  is the velocity profile that usually measured and compared to theory. It is evident from Fig. 3 that when the velocity profiles are scaled to the same boundary thickness, the  $m=0$  and  $m=0.1356$  solutions are very similar. On the other hand, the scaled  $v(x, y)$  velocity profiles given in Fig. 4 are very different.

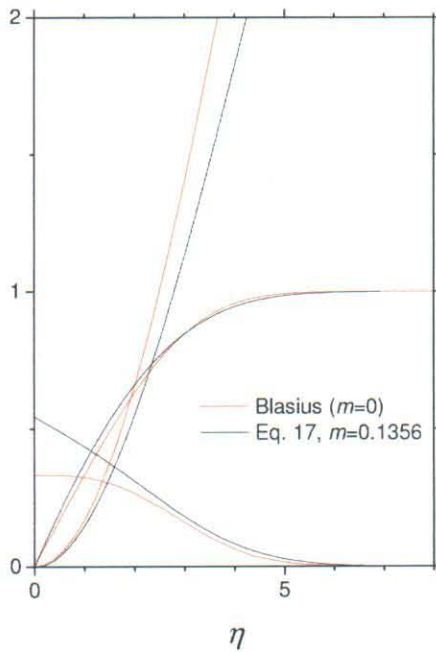


Fig. 2: The calculated results for  $f, f'$ , and  $f''$  for Eq. 17 with  $m=0$  and  $m=0.1356$ .

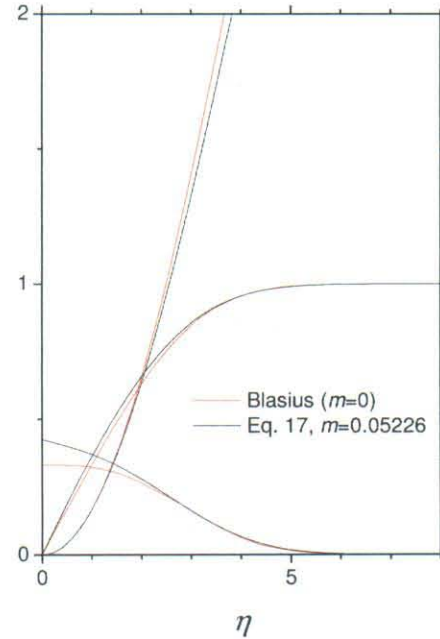


Fig. 5: The calculated results for  $f, f'$ , and  $f''$  for Eq. 17 with  $m=0$  and  $m=0.05226$ .



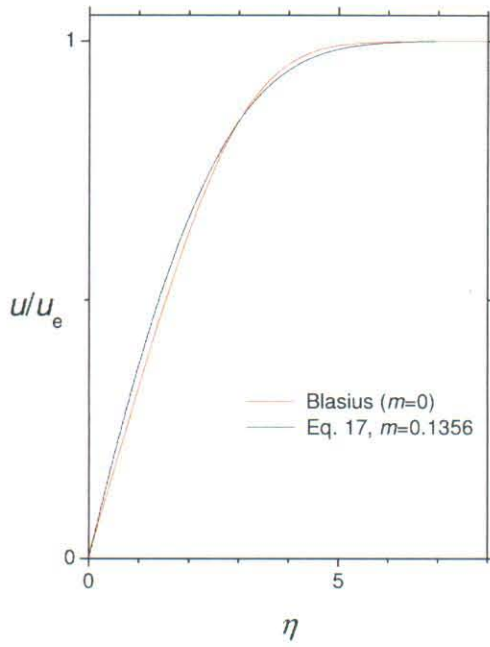


Fig. 3: The calculated results for  $u/u_e$  for Eq. 17 with  $m=0$  and  $m=0.1356$ .

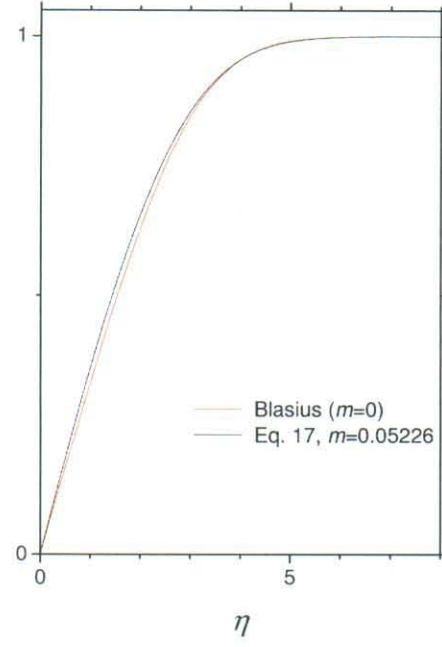


Fig. 6: The calculated results for  $u/u_e$  for Eq. 17 with  $m=0$  and  $m=0.05226$ .

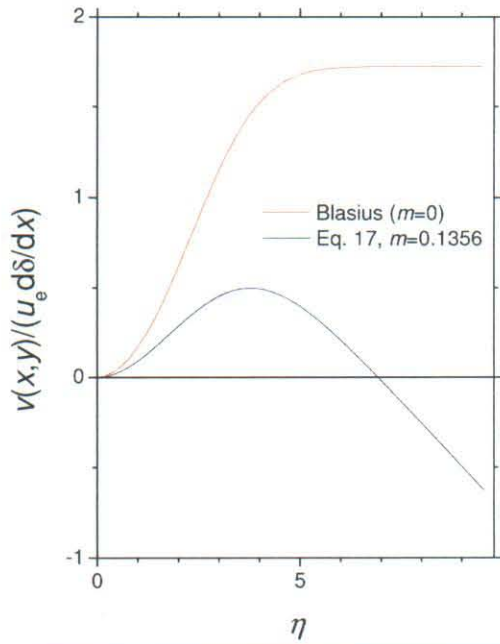


Fig. 4: The scaled velocity  $v(x,y)$  from Eq. 17 with  $m=0$  and  $m=0.1356$ .

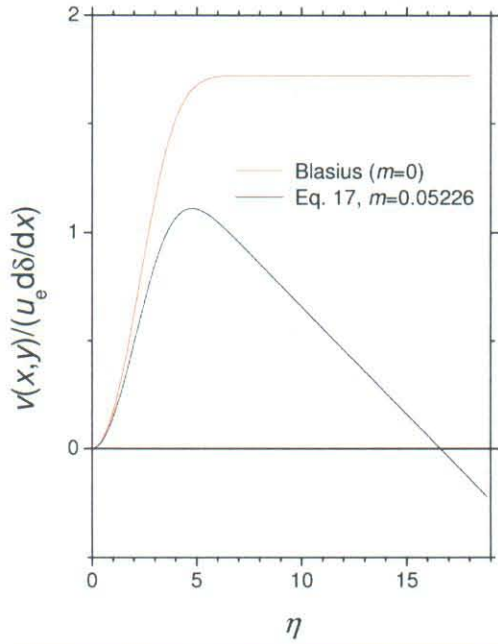


Fig. 7: The scaled velocity  $v(x,y)$  from Eq. 17 with  $m=0$  and  $m=0.05226$ .

## 7.2 Scenario 2

In this scenario we assumed that  $v(x, y)$  becomes zero much further into the free stream above the plate. A value of  $\eta_{v0} \cong 15$  was arbitrarily picked. Eq. 17 was solved by hand iterating the  $m$  value until the scaled  $v(x, y)$  velocity given in Eq. 22 is zero at  $\eta_{v0}$ . It was found that this occurred at  $m=0.05226$ . The results are shown in Figs. 5-7. For comparison, the Blasius solution is also shown. In making the comparison, it is necessary to scale one or the other solution so that they have the same boundary layer thickness. In Figs. 5-7, the  $m=0.05226$  solution  $\eta$  values are scaled such that the boundary thickness value is the same as the boundary thickness of the Blasius solution (the boundary layer thickness was calculated according to Weyburne [7]). The boundary layer thickness ratio was found to be 1.107. In Figs. 5-7, the  $m=0.05226$  solutions  $\eta$  values were multiplied by this 1.107 value.

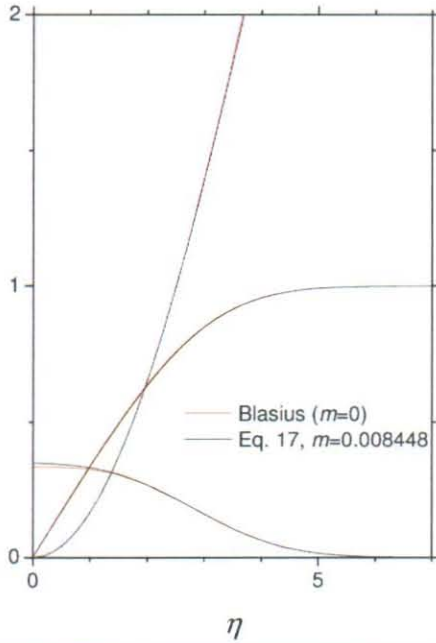


Fig. 8: The calculated results for  $f, f'$ , and  $f''$  for Eq. 17 with  $m=0$  and  $m=0.008448$ .

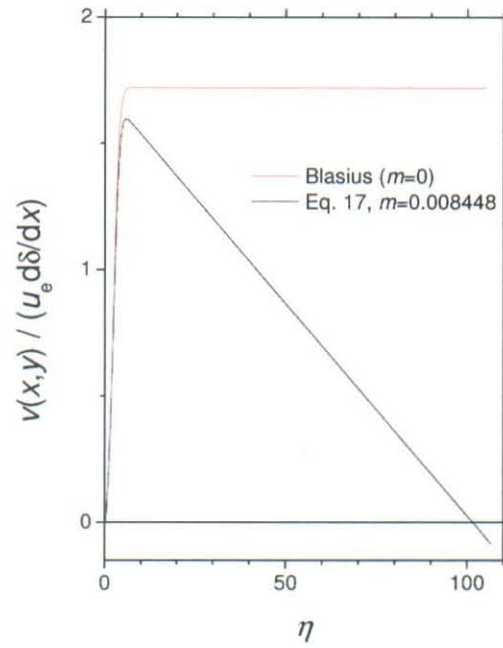


Fig. 9: The scaled velocity  $v(x, y)$  from Eq. 17 with  $m=0$  and  $m=0.008448$ .

## 7.3 Scenario 3

In this scenario we assumed that  $v(x, y)$  becomes zero at about 20 boundary thicknesses into the free stream above the plate. This corresponds to a value of  $\eta_{v0} \cong 100$ . Eq. 17 was again solved by hand iterating the  $m$  value until the scaled  $v(x, y)$  velocity given in Eq. 22 is zero at  $\eta_{v0}$ . It was found that this occurred at  $m=0.008448$ . The results are shown in Figs. 8 and 9. For comparison, the Blasius solution is also shown. In making the comparison, it is necessary to

scale one or the other solution so that they have the same boundary layer thickness. In Figs. 8 and 9, the  $m=0.008448$  solution  $\eta$  values are scaled such that the boundary thickness value is the same as the boundary thickness of the Blasius solution (the boundary layer thickness was calculated according to Weyburne [7]). The boundary layer thickness ratio was found to be 1.039. In Figs. 8 and 9, the  $m=0.008448$  solutions  $\eta$  values were multiplied by this 1.039 value.

Notice that in Fig. 8 that the Blasius solution (the  $m=0$  solution) and the  $m=0.008448$  solution lines fall on top of one another and are pretty much indistinguishable (at least for the  $f$  and  $f'$  cases). This means that once  $\eta_{v0}$  becomes on the order of 20 or more boundary layer thicknesses, the differences in the boundary layer profile for  $u(x,y)/u_e$  are probably too small to measure experimentally. However, note that the velocity  $v(x,y)$  (Fig. 9) still goes to zero and then negative as expected.

Two important parameters associated with the flow are the skin friction and pressure gradients. To calculate the skin friction, we start with the wall shear stress that is given by

$$\tau_0(x) = \mu \left. \frac{\partial u}{\partial y} \right|_{y=0} = \frac{\mu u_e}{\delta} f''|_{\eta=0} . \quad (25)$$

The skin friction coefficient then becomes

$$c_f = \frac{\tau_0}{\frac{1}{2} \rho u_e^2} = \frac{2\nu}{\delta u_e} f''|_{\eta=0} . \quad (26)$$

For the flow described above, a simple two parameter analytical fit yields

$$c_f = \frac{2 \sqrt{0.11026 + 1.38m}}{\sqrt{\frac{x u_e}{\nu}}} . \quad (27)$$

The actual the zero wall shear stress condition occurs at  $m=-0.090431$  in agreement with the Falkner-Skan results. The skin friction coefficient is difficult to measure experimentally. The pressure gradient along the flow direction on the plate, on the other hand, is relatively easy to measure. For the flow herein, the pressure gradient calculated using Eqs. 18 and 19 is given by

$$-\frac{1}{\rho} \frac{dp}{dx} = mb(x-x_0)^{2m-1} . \quad (28)$$

## 8. Discussion

The main intent of this research has been to find a realistic theoretical model for laminar flow over a flat plate. For the past one hundred years, it has been assumed that the Blasius flow model was this solution. However, we pointed out that the Blasius model falls short of what one would expect for laminar flow over a flat plate. The problem is that, contrary to expectations for flow over a flat plate, the Blasius model incorporates a zero pressure gradient. To address this



problem, we showed that it is possible to develop a more realistic theoretical model for flow over a flat plate that still retains the simplicity of the Blasius model. In the model developed above, the usual zero pressure gradient assumption was removed and replaced with a nonzero pressure gradient assumption. This allowed us to obtain a Falkner-Skan-type [4] similarity solution to the momentum equation. It is evident from Figs. 2-9 that for the most part, the Blasius solution and the new solutions for forced laminar flow over a flat plate are fairly similar. The biggest difference is in the velocity component perpendicular to the plate,  $v(x, y)$ . For the Blasius solution,  $v(x, y)$  asymptotes to a nonzero value that extends infinitely deep into the free stream above the plate whereas in the new model the velocity goes from positive to negative at a point somewhere in the free stream above the plate. Experimentally, it is not clear just where this occurs in a real fluid.

There has been 100 years of theoretical work on laminar flow on a flat plate based on the Blasius model. The Blasius model clearly does not represent the real flow situation for laminar flow over a flat plate nearly as well as the model proposed herein. A big question that needs to be answered is what are the theoretical implications of the new model? For example, how does a nonzero pressure gradient or higher skin friction coefficient affect laminar flow stability and laminar-turbulent transition? Clearly this will depend on the magnitude of the  $m$  value (Eq. 20). If, for a real fluid flow,  $m$  is small then the difference between the new model and the Blasius model will be small. Unfortunately, it is not presently possible to calculate  $m$  from available experimental datasets simply because there does not appear to be any experimental datasets available. It is not that it is difficult to do the measurement, it is just that no one has reported any of the measurements. Experimentally, it is relatively easy to measure the pressure gradient. For real fluids, the measured pressure gradient will have two components. One will be due to the displaced fluid from the development of the boundary layer and a second contribution due to the finite thickness of the flat plate. Experimental results seem to indicate that the finite thickness plate contribution is confined to the front of the plate which prevents flow similarity for the first 10-20% of the plate. If the velocity at the boundary layer edge can be measured after this initial non-similar region to obtain  $b$  and  $x_0$  (Eq. 21), then it should be possible to measure and fit the pressure gradient to Eq. 29 in order to extract the  $m$  value. With the  $m$  value in hand, it would then be possible to estimate the height above the plate where  $v(x, y)$  and the pressure gradient go to zero using Fig. 1. This would also make it possible to estimate the skin friction coefficient using Eq. 28. Once that data becomes available, it will be possible to evaluate the impact of the new model on laminar flow theory.

In Figs. 2-9, a comparison was made between the Blasius solution and the Falkner-Skan solution for various  $m$  values. In making the comparison, we noted that the boundary layer thicknesses for the two solutions are not the same. In fact, for the  $m=0.1356$  case the boundary thicknesses differ by 30% as determined by Weyburne [7]. However, we must point out that the scaling constant that is associated with the different  $\delta(x)$  values given by Eq. 18 are different in that the velocities are not the same. For the Blasius model, the associated velocity is  $u_\infty$  whereas for the Falkner-Skan model it is  $u_e$ . Since for this case  $u_e > u_\infty$ , the differences will be even larger than we have indicated. We will have to await experimental results to determine just how different the Blasius zero pressure gradient boundary layer thickness and the boundary layer thickness for a real laminar flow over a flat plate actually are.



The new model is based on the Falkner-Skan-type [4] momentum balance. Potential flow theory indicates that the free stream velocity over a wedge has a power-law functional form. This has led to the Falkner-Skan similarity solution to be associated with flow around a wedge. However, as we pointed out above, it is equally correct to interpret the equations in terms of flow on a flat plate with a pressure gradient. The difference in interpretation is emphasized by looking at Eq. 18 in which the power-law exponent  $m$  is given in terms of the pressure gradient. In most Falkner-Skan treatments in textbooks, the power-law exponent is usually interpreted in terms of a wedge angle  $\beta$  such that  $m = \beta/(2 - \beta)$ . The new interpretation advocated herein provides a valuable path to teach introductory students the concept of aerodynamic lift using a flat plate as a model for a wing. If one temporarily ignores the effects of the bottom of the plate, then one can describe lift in terms of the pressure gradient inducing a net inflow toward a pinned plate, or as an upward motion of the plate for an unpinned plate.

## 9. Conclusion

A Falkner-Skan-style theoretical model for flow over a flat plate was presented. The usual Blasius zero pressure gradient assumption is replaced with a nonzero pressure gradient assumption. This nonzero pressure gradient is what one should expect for laminar flow over a flat plate. By relaxing the Blasius pressure assumption and allowing a pressure gradient to develop along the flow direction on the plate, it is possible to obtain a flow solution for which the velocity flow perpendicular to plate goes to zero and then becomes negative at some finite location above the plate. This net inflow allows one to use the flat plate as a model for a wing with aerodynamic lift.

## References

- [1] H. Blasius, "Grenzschichten in Flüssigkeiten mit kleiner Reibung," *Zeitschrift für Mathematik und Physik*, **56**, 1(1908).
- [2] J. Jovanović, B. Frohnäpfel, E. Škaljić, and M. Jovanović, "Persistence of the Laminar Regime in a Flat Plate Boundary Layer at very High Reynolds Number," *Thermal Science*, **10**, 63(2006).
- [3] N. Patten, T. M. Young, and P. Griffin, "Design and Characteristics of New Test Facility for Flat Plate Boundary Layer Research," *Proc. World Acad. Sci., Eng. and Tech.*, **58**, 366(2008).
- [4] V. Falkner and S. Skan, "Some Approximate solutions of the boundary layer solutions," *Philosophical Magazine*, **12**, 865(1931).
- [5] H. Schlichting, *Boundary Layer Theory*, 7th ed., McGraw-Hill, New York, 1979.
- [6] K. Hiemenz, "Die Grenzschicht an einem in den gleichförmigen Flüssigkeitsstrom eingetauchten geraden Kreiszylinder," *Dingler's Polytech. J.*, **326**, 321(1911).

[7] D. Weyburne, "A mathematical description of the fluid boundary layer," *Applied Mathematics and Computation*, **175**, 1675(2006). Also D. Weyburne, Erratum to "A mathematical description of the fluid boundary layer," *Applied Mathematics and Computation*, **197**, 466(2008).